

Observation, analysis and modelling in complex fluid media

Two recent developments in numerical simulation of premixed and partially premixed turbulent flames

Luc Vervisch *, Pascale Domingo

INSA de Rouen, UMR-CNRS-6614-CORIA, campus du Madrillet, avenue de l'université, BP 8, 76801 Saint Étienne du Rouvray cedex, France

Available online 1 September 2006

Abstract

A subgrid scale closure for Large Eddy Simulation of premixed turbulent combustion (FSD-PDF) is proposed. It combines the Flame Surface Density (FSD) approach with a presumed Probability Density Function (PDF) of the progress variable that is used in flamelet chemistry tabulation. The FSD is useful to introduce in the presumed PDF the influence of the spatially filtered thin reaction zone evolving within the subgrid. This is achieved via the exact relation between the PDF and the FSD. In a second part, Direct Numerical Simulation of partially premixed combustion in a swirling flow is reported. The results are used to analyze the structure of the leading edge flame that ensures flame stabilization. *To cite this article: L. Vervisch, P. Domingo, C. R. Mecanique 334 (2006).*

© 2006 Académie des sciences. Published by Elsevier SAS. All rights reserved.

Résumé

Deux développements récents en simulation numérique de flammes turbulentes en combustion prémélangée et partiellement prémélangée. Un modèle de fermeture sous maille pour des simulations des grandes échelles de combustion turbulente prémélangée (FSD-PDF) est proposé. Il combine l'approche de Densité de Surface de Flamme (FSD) avec une densité de probabilité présumée (PDF) pour la variable qui traduit l'avancement de la réaction dans la tabulation utilisée pour la chimie. La méthode FSD est utile pour introduire dans la PDF présumée l'influence de la zone fine de réaction filtrée spatialement qui évolue à l'intérieur de la sous-maille. Ceci est obtenu via la relation exacte qui lie la PDF et la FSD. Dans une seconde partie, des résultats de Simulation Numérique Directe (DNS) pour de la combustion partiellement prémélangée dans un écoulement avec rotation (*swirl*) sont reportés. Les résultats sont utilisés pour analyser la structure de la flamme de bord d'entrée qui assure la stabilisation de la flamme. *Pour citer cet article : L. Vervisch, P. Domingo, C. R. Mecanique 334 (2006).*

© 2006 Académie des sciences. Published by Elsevier SAS. All rights reserved.

Keywords: Turbulence; Combustion; Flames; Numerical simulation

Mots-clés: Turbulence; Combustion; Flammes; Simulation numérique

* Corresponding author.

E-mail addresses: vervisch@coria.fr (L. Vervisch), domingo@coria.fr (P. Domingo).

1. Introduction

Direct Numerical Simulation (DNS) and Large Eddy Simulation (LES) of turbulent flames are very rapidly growing tools, mainly because of the progress of turbulent combustion modeling, numerics and computer science. Two recent developments in DNS [1] and LES [2], presented on the occasion of Roland Borghi sixtieth birthday, are discussed. LES of premixed turbulent combustion is first addressed. LES resolves the unsteady coherent large scales observed in turbulent flows, after removing small scales by filtering in space. Accordingly, the smallest scales must be modeled. The presumed Probability Density Function (PDF) framework discussed by Borghi [3] is adopted to describe this small scale activity. The ratio Δ/δ_L , between the filter size and the characteristic thickness of the premixed flame that evolves within the subgrid, is one of the important ingredients of LES of premixed turbulent combustion. It is shown how this key information on flame length scale can be introduced into the PDF and some LES results are compared with measurements.

The second part deals with Direct Numerical Simulation (DNS) of partially premixed turbulent combustion in swirling flows. DNS resolves the full range of flow scales and very detailed information is made available to progress in the understanding of leading edge flames propagation in rotating flows.

2. LES of premixed turbulent combustion

It is proposed to capture the SubGrid Scale (SGS) behavior of the thin premixed flame from three control parameters: A filtered reaction progress variable \tilde{c} ($c = 0$ in fresh gases and $c = 1$ in fully burnt products), its SGS variance $\tilde{c}_v = \tilde{c}c - \tilde{c}\tilde{c}$, and, $\overline{G}_\Delta(c)$, a filtered reference distribution of spatial gradient of that progress variable. These three quantities are used to presume $\tilde{P}(c^*; \underline{x}, t)$, the PDF of the progress variable. Once the PDF is approximated, all SGS terms related to chemistry (filtered species and filtered chemical sources) may be computed as:

$$\tilde{\Phi}(\underline{x}, t) = \int_0^1 \Phi^{\text{FPI}}(c^*) \tilde{P}(c^*; \underline{x}, t) dc^* \quad (1)$$

where $\Phi^{\text{FPI}}(c^*)$ is the value of the quantity Φ in the FPI [4] flamelet tabulation of detailed chemistry with the progress variable c .

Because in LES $\Delta/\delta_L \gg 1$, the flame is weakly resolved and the PDF features a shape close to its Bi-Modal-Limit, as in BML RANS modeling [5]:

$$\tilde{P}(c^*; \underline{x}, t) = \alpha(\underline{x}, t)\delta(c^*) + \beta(\underline{x}, t)\delta(1 - c^*) + F(c^*; \underline{x}, t) \quad (2)$$

where the function $F(c^*; \underline{x}, t)$ depends on the SGS statistical properties of the iso- c^* surfaces evolving between $c^* = 0$ and $c^* = 1$. The accuracy of the prediction of the PDF in this internal part of the flame is crucial since intermediate species present in detailed chemistry feature strong variations in this zone. The link between $\Sigma(c^*; \underline{x}, t)$, the Flame Surface Density (FSD), and the PDF may be introduced to complete the closure. $\Sigma(c^*; \underline{x}, t)$ is related to the SGS PDF by [6]:

$$\tilde{P}(c^*; \underline{x}, t) = \frac{\Sigma(c^*; \underline{x}, t)}{(|\nabla c| |c^*)} \quad (3)$$

In this last expression, $\Sigma(c^*; \underline{x}, t)$ the FSD depends on the iso-surface c^* via the conditional average of the gradient ($|\nabla c| |c^*$). In premixed combustion, because the flame is locally thin, it is usually assumed that within the range $0 < c^* < 1$, species iso-surfaces stay mostly parallel to each other, a behaviour confirmed by DNS [7]. $\Sigma(c^*; \underline{x}, t)$ thus weakly varies in the internal part of the diffusive-reactive layer and one may write $\Sigma(c^*; \underline{x}, t) \approx \sigma(\underline{x}, t)$, where $\sigma(\underline{x}, t)$ does not depend on c^* . $\sigma(\underline{x}, t)$ characterises the amplitude of the FSD, which strongly depends on the magnitude of subgrid scale flame wrinkling and on the level of flame resolution. Combining those observations with Eq. (3), it is proposed to approximate the function $F(c^*; \underline{x}, t)$ of the PDF (Eq. (2)) in the form:

$$F(c^*; \underline{x}, t) = \frac{\sigma(\underline{x}, t)}{\overline{G}_\Delta(c^*)} H(c^*) H(1 - c^*) \quad (4)$$

The Heaviside function is introduced to limit the contribution of $F(c^*; \underline{x}, t)$ to the internal part of the composition space ($0 < c^* < 1$). $\overline{G}_\Delta(c^*)$ approximates $(|\nabla c|/c^*)$ as a gradient distribution measured from the reference planar and unstrained FPI flamelet that has been filtered at the level Δ :

$$\overline{G}_\Delta(c(x)) = \int_{-\infty}^{+\infty} |\nabla c|^{\text{FPI}} F_\Delta(x - x') dx' \tag{5}$$

where F is the LES filter of size Δ . Eq. (4) therefore appears as a possible candidate to inform the PDF on the scale at which the flame is seen by the coarse LES grid. Combining Eq. (2) with Eq. (4), the SGS progress variable FSD-PDF reads:

$$\tilde{P}(c^*; \underline{x}, t) = \alpha(\underline{x}, t)\delta(c^*) + \beta(\underline{x}, t)\delta(1 - c^*) + \frac{\sigma(\underline{x}, t)}{\overline{G}_\Delta(c^*)} H(c^*)H(1 - c^*)$$

The presumed PDF relies on three parameters, α , β and σ . They may be determined at every location and instant in time from three constraints that the PDF must fulfil:

$$\int_0^1 \tilde{P}(c^*) dc^* = 1; \quad \int_0^1 c^* \tilde{P}(c^*) dc^* = \tilde{c}; \quad \int_0^1 c^{*2} \tilde{P}(c^*) dc^* = \tilde{c}^2 \tag{6}$$

These three equations bring the relations:

$$\alpha + \beta + a\sigma = 1; \quad \beta + b\sigma = \tilde{c}; \quad \beta + d\sigma = S\tilde{c}(1 - \tilde{c}) + \tilde{c}^2 \tag{7}$$

where $S = \tilde{c}_v/\tilde{c}(1 - \tilde{c})$ represents the unmixedness computed from the rms of c . The coefficients a , b and d are fully determined from:

$$a = \int_\varepsilon^{1-\varepsilon} \frac{1}{\overline{G}_\Delta(c^*)} dc^*; \quad b = \int_\varepsilon^{1-\varepsilon} \frac{c^*}{\overline{G}_\Delta(c^*)} dc^*; \quad d = \int_\varepsilon^{1-\varepsilon} \frac{c^{*2}}{\overline{G}_\Delta(c^*)} dc^* \tag{8}$$

ε is a small parameter used to define the inner zone of the premixed flamelet in composition space, $\varepsilon = 0.001$ was retained in this study. Tests have been performed where this parameter was slightly varied, LES results are not strongly affected as long as $\varepsilon < 0.01$. After straightforward manipulations, the coefficients of the presumed PDF are determined from the filtered progress variable and corresponding SGS variance expressed in terms of unmixedness:

$$\alpha = (1 - \tilde{c}) - \left(\frac{a - b}{b - d}\right)(1 - S)\tilde{c}(1 - \tilde{c})$$

$$\beta = \tilde{c} - \left(\frac{b}{b - d}\right)(1 - S)\tilde{c}(1 - \tilde{c})$$

$$\sigma = \left(\frac{1}{b - d}\right)(1 - S)\tilde{c}(1 - \tilde{c})$$

These relations fail for negative values of α or β . Leading to the additional constraints:

$$S > 1 - \left(\frac{b - d}{a - b}\right)\frac{1}{\tilde{c}}; \quad S > 1 - \left(\frac{b - d}{b}\right)\frac{1}{1 - \tilde{c}} \tag{9}$$

Consequently, the SGS presumed PDF proposed in Eq. (6) cannot be used for low values of the unmixedness (i.e., small levels of \tilde{c}_v). For moderate levels of SGS fluctuations, the shape of the SGS PDF is expected to be much less crucial, as it is used to average over values that are close to the filtered level \tilde{c} . Among the available options, a Beta-PDF [8] is retained to deal with points having low level of SGS variance.

The ORACLES experiment was specifically designed for LES validation by Nguyen and Bruel [9] at CNRS in Poitiers. It consists of two channels of fully premixed mixtures separated by a splitter plate and exposed to a sudden expansion. The channels are 3 meters long to obtain a fully developed turbulent channel flow. The combustion chamber is located after the sudden expansion and is 2 meters long with insulated walls. The outlet was carefully set to monitor the outflow rate of the rig ($3.5 \text{ m}^3/\text{s}$). The bulk velocity is of the order of $U_d = 11.0 \text{ m/s}$. The Reynolds number

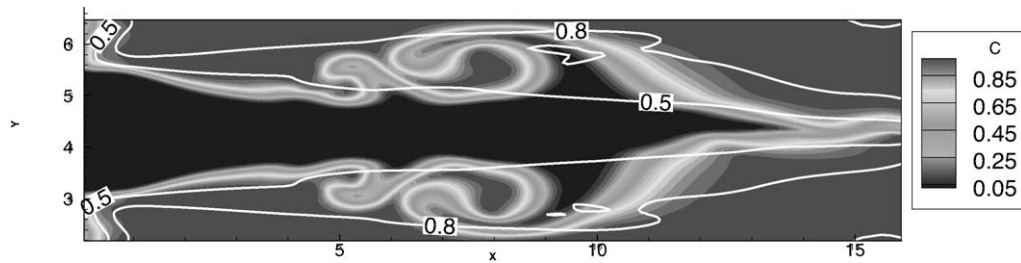


Fig. 1. Instantaneous and time-averaged progress variable iso-contours. Gray scale: Two-dimensional cut of the instantaneous field. White line: Time average. x and y are normalized by h .

Fig. 1. Iso-contours de la variable d'avancement instantanée et moyennée dans le temps. Échelle de gris : Coupe bi-dimensionnelle du champ instantané. Ligne blanche : Moyenne temporelle. x et y sont normalisés par h .

estimated from U_d , the height of the inlet channel $H = 30.4$ mm and the viscosity of fresh mixture at the reference temperature $T_0 = 276$ K, is of the order of 25 000. In the transverse direction, the depth of the channel is 150.5 mm. The flame is stabilised in the shear layers that develop after the sudden expansion and transverse distributions of mean velocity measurements are available at various streamwise locations. The reported simulation focusses on the case where the equivalence ratio is 0.75 in both streams.

The fully compressible set of Navier–Stokes equations together with the balance equations for \tilde{c} and $\tilde{\varphi}_v = \tilde{c}(1 - \tilde{c}) - \tilde{c}_v$ [2] are solved using a fourth order finite volume skew-symmetric-like scheme proposed by Ducros et al. [10] for the spatial derivatives. This scheme was specifically developed and tested for LES, it is combined with a second order Runge–Kutta explicit time stepping. Because the equations are solved in their fully compressible form, the time step limitation includes acoustic waves and Navier–Stokes Characteristic Boundary Conditions [11] are retained.

The unsteady behavior of the ducted flame was carefully identified and calibrated by time series measurements [9]. For the case studied, a specific acoustic mode with large scale fluctuations at a characteristic frequency of the order of 50 Hz was found. To avoid simulating the full system, preliminary simulations of the channel flows, upstream of the main combustion chamber, were performed to generate proper inlet conditions. They are then perturbed according to the spectrum experimentally measured in the inlet plane of the combustion chamber [9], right after the splitter plate. The measured power density spectrum of the longitudinal velocity component exhibits a peak at 50 Hz. In the simulations, a sinusoidal forcing at this specific frequency is added to the velocity inlet to mimic the corresponding acoustic mode. Following this procedure, only 450 mm long of the facility is computed, just after the sudden expansion with a spanwise length of 70 mm. The three-dimensional non-uniform grid is composed of $128 \times 96 \times 32$ nodes. In the region where the flame develops, the grid is such that $\Delta/\delta_L \approx 20$ and this value is retained in the FSD-PDF for the filtered gradient \overline{G}_Δ (Eq. (5)). To construct mean values, instantaneous LES fields are cumulated over twice the time elapsed when a fluid particle travels from inlet to outlet.

Fig. 1 presents an instantaneous field of \tilde{c} , the iso-lines of the time averaged filtered progress variable are also displayed for the values 0.5 and 0.8. Figs. 2 and 3 show distributions of time average filtered streamwise, transverse, and RMS velocity. Most of the reacting flow structure is well reproduced, especially the streamwise velocity that is correctly estimated. The quality of the prediction is slightly reduced in the spanwise direction at the streamwise location $x/h = 10$, but the overall distribution follows the measurements. The level of RMS velocity is also in agreement with experiment. This preliminary test of FSD-PDF is thus encouraging.

3. DNS of partially premixed flame in a swirling flow

Flow rotation is used to favor flame stabilization in many premixed or non-premixed combustion systems [12]. A synthetic Direct Numerical Simulation (DNS) model problem is now proposed to progress in the understanding of the basic mechanisms contributing to partially premixed flame propagation in such a rotating flow. A turbulent columnar vortex (Fig. 4) carrying a non-premixed distribution of fuel and oxidizer is sent towards a planar and stoichiometric premixed flame that is initially steady. The fuel and air distribution is so that pure fuel is found in the core of the vortex that evolves within an air environment. The flow is progressing at the laminar flame burning velocity S_L in the x direction towards the planar y – z flame. The characteristic radius of the swirling flow is $R_v \approx 20\delta_L$, where δ_L is the thermal

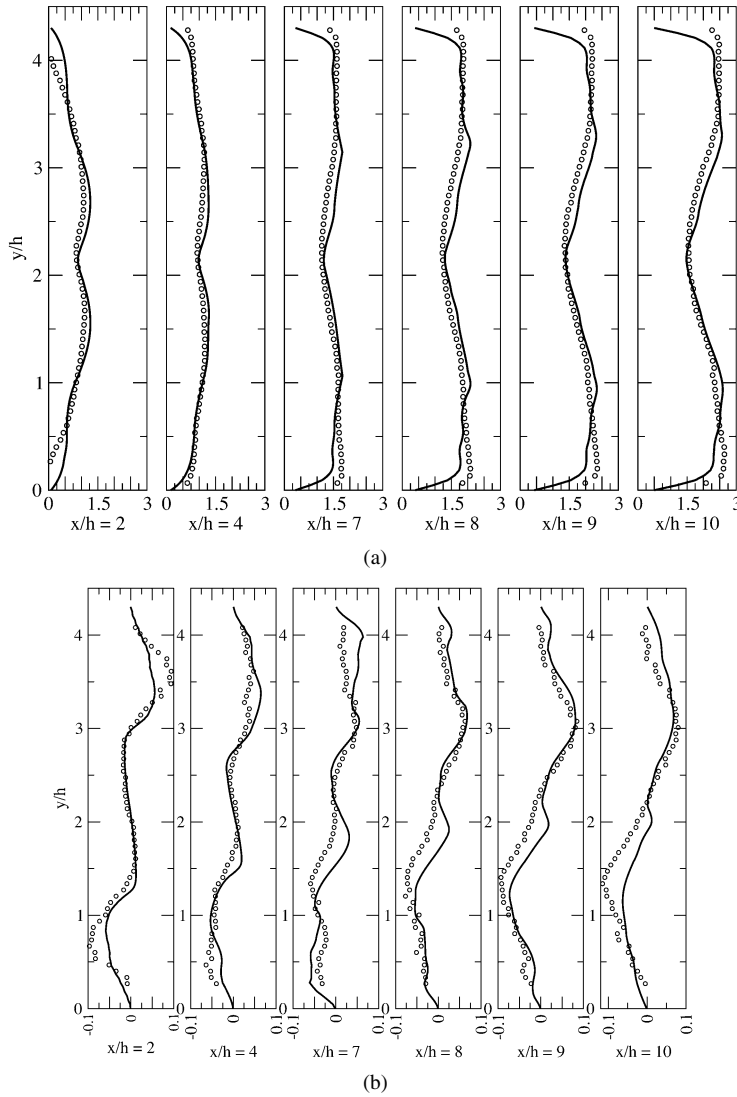


Fig. 2. Transverse distribution of time averaged velocity component. (a): Streamwise, (b): Spanwise. Symbol: ORACLE experiment. Line: LES.
 Fig. 2. Distributions transversales des composantes de vitesse moyennées dans le temps. (a) Longitudinale. (b) Transversale. Symbole : Expérience ORACLE. Ligne : LES.

thickness of the stoichiometric premixed flame. The stoichiometric surface is located at a distance $0.90R_V$ measured from the axis of mean flow rotation. The size of the computational domain is about $8R_V$ in every direction and a mesh of 4 300 000 points is used. Previously established combustion DNS techniques are adopted [13,14]. The ratio between the characteristic turbulent velocity fluctuations and the burning velocity is $u'/S_L = 5$. The Reynolds number, based on the Taylor scale, of the turbulence is of the order of 16. The ratio between the maximum circumferential flow velocity and the flame speed is $V_v/S_L = 20$.

In all cases simulated, the flame moves upstream of its initial position after penetrating the turbulent vortex to propagate against the incoming flow. As expected, rotation and turbulence are associated to a flame displacement velocity that is larger than S_L . Fig. 5 illustrates this rapid partially premixed flame propagation. It shows snapshots of the iso-temperature surface $T^* = 0.8T_b$, where T_b is the temperature of the stoichiometric burnt gases, which is five time larger than the one of the fresh mixture. A phenomenon having similarities with flash-back in non-premixed swirl burner is observed [15,16]. Very soon after the beginning of the interaction between the flame and the incoming swirling flow, burnt gases are found inside the core of the tubular vortex, thereby upstream of the initial reaction zone

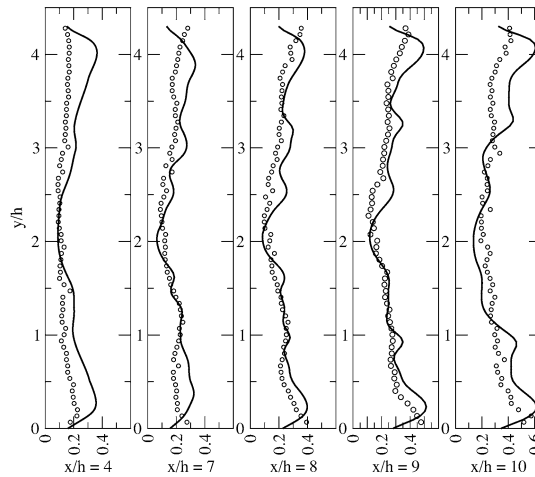


Fig. 3. Transverse distribution of time averaged RMS velocity. Symbol: ORACLES experiment. Line: LES.

Fig. 3. Distribution transversale de la valeur RMS de la vitesse obtenue par moyenne dans le temps. Symbole : Expérience ORACLES. Ligne : LES.

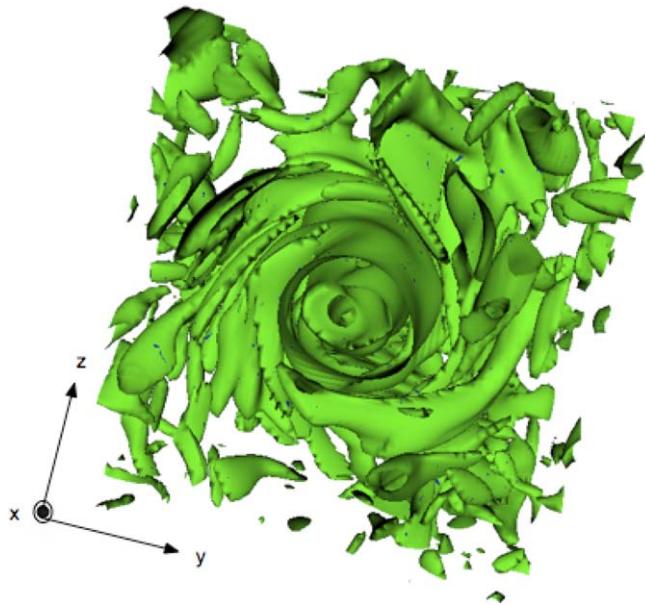


Fig. 4. Snapshot of the vorticity field progressing towards the flame.

Fig. 4. Instantané du champ de vorticit  progressing vers la flamme.

position (i.e., in the fresh gas side). The strongly burning leading flame that subsequently develops and propagates inside the rotating flow takes the shape of a disturbed torus that follows a swirling movement. When penetrating the turbulent columnar spinning flow in which there is a pressure drop, the flame develops a precursor azimuthal vortex that accelerates the propagation of the reaction zone by inducing a forward velocity at the flame tip. A mechanism that was previously reported in the literature and analyzed in the fully premixed case without turbulent velocity fluctuations [17–19]. A vorticity torus is observed ahead of the leading flame resulting from the radial expansion of the tubular vortex because of heat release. This torus of vorticity behaves as a wave that propagates slightly upstream of the leading edge of the reaction zone. It is a byproduct of the density jump attached to the flame surface.

Fig. 6 shows iso-lines of the burning rate (energy source) and of the stoichiometric line when the reaction zones propagate inside the rotating flow. In Fig. 6 (left), the cut is taken in a x – z plane passing by the vortex center. The

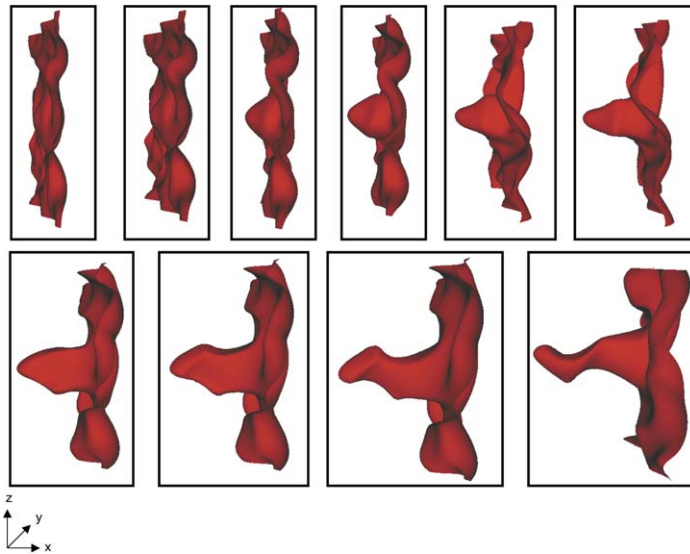


Fig. 5. Time evolution of the iso-temperature surface $T^* = 0.8T_b$. Time elapsed between two frames: $\Delta t = 0.66(R_v/V_v)$.

Fig. 5. Evolution temporelle de la surface d'iso-température $T^* = 0.8T_b$. Intervalle de temps entre deux images : $\Delta t = 0.66(R_v/V_v)$.

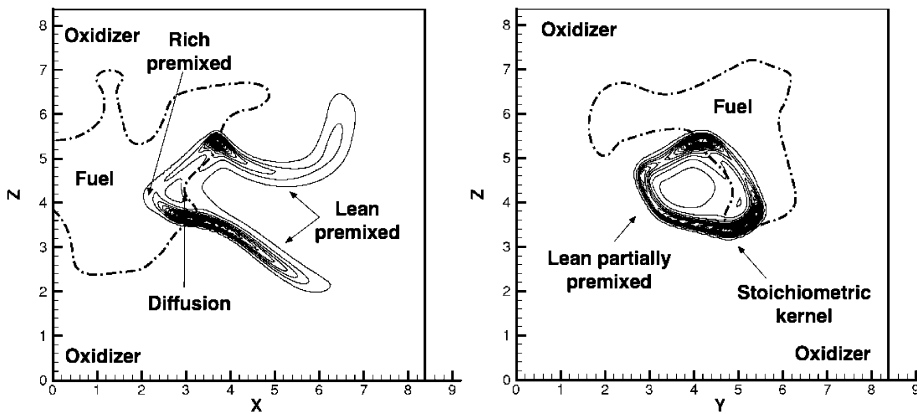


Fig. 6. Line: Iso-lines of burning rate (energy source). Dash line: Stoichiometric contour. Left: In a $x-z$ plane passing by the turbulent tubular vortex center. Right: In a $y-z$ plane located at $x = 3.77R_v$.

Fig. 6. Ligne : Iso-lignes du taux de réaction (source d'énergie). Ligne pointillée : Contour stoichiométrique. Gauche : Dans un plan $x-z$ passant par le centre du tourbillon tubulaire. Droite : Dans un plan $y-z$ situé à $x = 3.77R_v$.

flame is seen under a different angle of view in Fig. 6 (right), which displays the same information but in a $y-z$ plane located at $x = 3.77R_v$. (The origin of the coordinate is located at the initial planar flame position.) The flame index based on species gradient [13] was used to delineate between premixed and diffusion burning (not shown). A ring of reaction zone attached to the stoichiometric line is burning in a partially premixed mode (Fig. 6 (left)). Inside this ring associated to the vorticity torus discussed before, fuel and oxidizer are mixed with products to weakly burn in a diffusive regime. In a given $y-z$ plane, a portion of the premixed ring is always stoichiometric. The remaining part of it is controlled by a flame developing in a mixture whose equivalence ratio is weakly varying. This flame evolves in time from lean to rich when it propagates according to the swirling movement. Slightly upstream of the burning ring ($2 < x < 3$ in Fig. 6) a rich premixed flame is observed, and downstream ($5 < x < 7$) two trailing lean premixed flames subsist.

The velocity u_{fl} of the fluid flowing through the reaction zone may be obtained in the DNS from $u_{fl} = -\mathbf{u} \cdot \mathbf{n}$, where \mathbf{u} is the velocity vector and $\mathbf{n} = -\nabla c/|\nabla c|$ the normal to the flame front. The progress variable c of the

partially premixed flame ($c = 0$ in fresh gases and unity in fully burnt products) is defined as in previous DNS studies [13]. $u_{fl} > 0$ (respectively $u_{fl} < 0$) means that the fluid flows through the flame from fresh to burnt gases (respectively from burnt to fresh). High probability of the occurrence $u_{fl} \approx S_L$ is found, the condition representative of local stoichiometric premixed flame propagation in the non-premixed turbulent flow.

A careful examination of the time evolution of the partially premixed flame ring shown in Fig. 6 has also been performed. Depending on the flow conditions, every given burning point over this ring is subjected to a succession of flame freely propagating ($u_{fl} \approx S_L$) and strong flow advection ($|u_{fl}| > S_L$). While in the vicinity of the centerline axis, where the rich flame is found (Fig. 6), the reaction zone is sucked upstream due to the pressure drop in the core of the tubular vortex. This combination over time of movement along the vortex axis associated to the circumferential motion along the stoichiometric surface results in the overall non-premixed swirling flame propagation.

4. Summary

A novel presumed Probability Density Function strategy is first discussed for LES, in which the basic relation between the PDF and the Flame Surface Density is used. The objective is to introduce into the presumed PDF some information on the characteristic premixed flame that is filtered by the LES grid. To validate the full procedure, three dimensional LES of a given case of the ORACLES experiment (flames stabilized in a sudden expansion) is computed and results are compared with available measurements.

In a second part, Direct Numerical Simulation (DNS) of flames propagating in a turbulent columnar vortex are performed. The exact structure of the spinning partially premixed flame obtained with non-premixed injection is analyzed. It is composed of an upstream rich premixed flame, followed by a partially premixed ring containing premixed kernels at stoichiometric condition that follow the flow streamlines, leading to a swirling upstream movement of the overall leading edge flame. A diffusion flame is observed in the core of the partially premixed ring. It separates fuel left behind the rich premixed flame from oxidizer strongly diluted with burnt products.

References

- [1] P. Domingo, L. Vervisch, DNS of partially premixed flame propagating in a turbulent rotating flow, in preparation.
- [2] P. Domingo, L. Vervisch, S. Payet, R. Hauguel, DNS of a premixed turbulent v-flame and LES of a ducted-flame using a FSD-PDF subgrid scale closure with FPI tabulated chemistry, *Combust. Flame* 134 (4) (2005) 566–586.
- [3] R. Borghi, Turbulent combustion modelling, *Prog. Energy Combust. Sci.* 14 (1988) 245–292.
- [4] B. Fiorina, R. Baron, O. Gicquel, D. Thevenin, S. Carpentier, N. Darabiha, Modelling non-adiabatic partially premixed flames using flame-prolongation of ILDM, *Combust. Theory Model.* 7 (3) (2003) 449–470.
- [5] K.N.C. Bray, The challenge of turbulent combustion, *Proc. Combust. Inst.* 26 (1996) 1–26.
- [6] L. Vervisch, E. Bidaux, K.N.C. Bray, W. Kollmann, Surface density function in premixed turbulent combustion modeling, similarities between probability density function and flame surface approaches, *Phys. Fluids* 7 (10) (1995) 2496–2503.
- [7] L. Vervisch, W. Kollmann, K.N.C. Bray, Dynamics of iso-concentration surfaces in premixed turbulent flames, in: *Tenth Symposium on Turbulent Shear Flows*, 1995, number 22-1.
- [8] P.A. Libby, F.A. Williams, Turbulent combustion: Fundamental aspects and a review, in: P.A. Libby, F.A. Williams (Eds.), *Turbulent Reacting Flows*, Academic Press, London, 1994, pp. 2–61.
- [9] P.D. Nguyen, P. Bruel, Turbulent reacting flow in a dump combustor: experimental determination of the influence of the inlet equivalence ratio difference on the contribution of the coherent and stochastic motions to the velocity field dynamics, in: *41st Aerospace Sciences Meeting and Exhibit*, Reno, USA, January 2003, AIAA, 2003, Paper 2003-0958.
- [10] F. Ducros, F. Laporte, T. Soulères, V. Guinot, P. Moinat, B. Caruelle, High-order fluxes for conservative skew-symmetric-like schemes in structured meshes: application to compressible flows, *J. Comput. Phys.* 161 (2000) 114–139.
- [11] T. Poinso, S.K. Lele, Boundary conditions for direct simulations of compressible viscous flows, *J. Comput. Phys.* 1 (101) (1992) 104–129.
- [12] C. Schneider, A. Dreizler, J. Janicka, Fluid dynamical analysis of atmospheric reacting and isothermal swirling flows, *Flow Turbulence Combust.* 74 (1) (2005) 103–127.
- [13] P. Domingo, L. Vervisch, J. Réveillon, DNS analysis of partially premixed combustion in spray and gaseous turbulent-flame bases stabilized in hot air, *Combust. Flame* 140 (3) (2005) 172–195.
- [14] J. Réveillon, L. Vervisch, Analysis of weakly turbulent diluted-spray flames and combustion regimes, *J. Fluid Mech.* 537 (2005) 317–347.
- [15] W.J. Sheu, S.H. Sohrab, G.I. Sivashinsky, Effect of rotation on Bunsen flame, *Combust. Flame* 79 (2) (1990).
- [16] Y. Sommerer, D. Galley, T. Poinso, S. Ducruix, S. Veynante, Les of flashback and extinction in a swirled burner, *J. Turbulence* 5 (1) (2004).
- [17] A. Umemura, K. Tomita, Rapid flame propagation in a vortex tube in perspective of vortex breakdown phenomena, *Combust. Flame* 125 (1/2) (2001) 820–838.
- [18] T. Hasegawa, R. Nakamichi, S. Nishiki, Mechanism of flame evolution along a fine vortex, *Combust. Theory Model.* 6 (3) (2002) 413–424.
- [19] W.T. Ashurst, *Combust. Sci. Technol.* 112 (1996) 175–185.